HHS Public Access

Author manuscript

Arch Toxicol. Author manuscript; available in PMC 2017 September 01.

Published in final edited form as:

Arch Toxicol. 2016 September ; 90(9): 2187–2200. doi:10.1007/s00204-015-1600-z.

2,3,5,6-Tetramethylpyrazine (TMP) down-regulated arsenic-induced heme oxygenase-1 and ARS2 expression by inhibiting Nrf2, NF-κB, AP-1 and MAPK pathways in human proximal tubular cells

Xuezhong Gong[a,b,*], **Vladimir N. Ivanov**[b], and **Tom K. Hei**[b,c]

[a]Department of Nephrology, Shanghai Municipal Hospital of Traditional Chinese Medicine, Shanghai University of Traditional Chinese Medicine, 274 Zhijiang Middle Road, Shanghai 200071, China

[b]Center for Radiological Research, College of Physician and Surgeons, Columbia University, 630 West 168th Street, NY 10032, United States

[c]Department of Radiation Oncology, College of Physician and Surgeons, Columbia University, 630 West 168th Street, NY 10032, United States

Abstract

Our recent study demonstrated that sodium arsenite at a clinically relevant dose induced nephrotoxicity in human renal proximal tubular epithelial cell line HK-2, which could be inhibited by natural product 2,3,5,6-Tetramethylpyrazine (TMP) with antioxidant activity. The present study demonstrated that arsenic exposure resulted in protein and enzymatic induction of heme oxygenase-1 (HO-1) in dose- and time-dependent manners in HK-2 cells. Blocking HO-1enzymatic activity by Zinc protoporphyrin (ZnPP) augmented arsenic-induced apoptosis, ROS production and mitochondrial dysfunction, suggesting a critical role for HO-1 as a renal protectant in this procession. On the other hand, TMP, upstream of HO-1, inhibited arsenic-induced ROS production and ROS-dependent HO-1 expression. TMP also prevented mitochondria dysfunction and suppressed activation of the intrinsic apoptotic pathway in HK-2 cells. Our results revealed that the regulation of arsenic-induced HO-1 expression was performed through multiple ROS-dependent signal pathways and the corresponding transcription factors, including p38 MAPK and JNK (but not ERK), AP-1, Nrf2 and NF-κB. TMP inhibited arsenic-induced activations of JNK, p38 MAPK, ERK, AP-1 and Nrf2 and block HO-1 protein expression. The present study, furthermore, demonstrated arsenic-induced expression of Arsenic response protein 2 (ARS2) that was regulated by p38 MAPK, ERK and NF-κB. To our knowledge, this is the first report showing that ARS2 involved in arsenic-induced nephrotoxicity while TMP pretreatment prevented such an up-regulation of ARS2 in HK-2 cells. Given ARS2 and HO-1 sharing the similar regulation mechanism, we speculated that ARS2 might also mediate cell survival in this procession. In summary, our study highlighted a role of HO-1 in the protection against arsenic-induced

[*]Corresponding author: 274 Zhijiang Middle Road, Shanghai Municipal Hospital of Traditional Chinese Medicine, 200071, Shanghai, China. Tel.: +86 21 56639828-3102; Fax: +86 21 56639310; shnanshan@hotmail.com.

Conflict of interest: The authors declare that they have no conflict of interest.

cytotoxicity downstream from the primary targets of TMP and further indicated that TMP may be used as a potential therapeutic agent in the treatment of arsenic-induced nephrotoxicity.

Keywords

Sodium arsenite; tetramethylpyrazine (TMP); nephrotoxicity; mitochondrial dysfunction; inducible heme oxygenase-1 (HO-1); arsenic response protein 2 (ARS2); nuclear factor erythroid derived-2 (Nrf2)

Introduction

Arsenic (*As*) is an important environmental contaminant affecting more than 140 million people worldwide through contaminated drinking water (Rodriguez-Lado et al. 2013). Recent epidemiologic studies in a rural United States population, in some regions of China, and especially, in Bangladesh, suggest arsenic is a major risk factor for kidney disease (Chen et al. 2011; Zheng et al. 2013). Kidney is one of the targeted organs of arsenic cytotoxicity that could cause renal dysfunction, proteinuria and chronic kidney disease (CKD) (Yu et al. 2013; Michael 2013; Ruiz-Hernandez et al. 2015; Zheng et al. 2014; Chen et al. 2014). Our recent study demonstrated that sodium arsenite at a clinically relevant dose induced cytotoxicity in human renal proximal tubular epithelial cell line, HK-2, which served as a representative cell model for exposures of the human kidney to *As*, drug-induced nephrotoxicity, and acute kidney injury (Huang et al. 2015; Peraza et al. 2003; Peraza et al. 2006; Wang et al. 2013b). Furthermore, our recent results indicated that such a nephrotoxicity was associated with a dramatic increase in intracellular ROS production, mitochondrial dysfunction, inflammation, apoptosis and autophagy (Gong et al. 2014). However, the precise molecular mechanisms responsible for arsenic nephrotoxicity remain largely unclear.

The inducible heme oxygenase-1 (HO-1), could exhibit anti-apoptotic, anti-oxidative and anti-inflammatory properties and thus be a renal protectant in multiple kidney injuries, such as acute kidney injury (AKI) induced by ischemia or nephrotoxicity induced by cisplatin and contrasting solutions (Chang et al. 2014; Miyagi et al. 2014). The critical role of HO-1 has also been reported in several organ injuries (Wang and Dore 2007; Billings et al. 2014). Given HO-1 also has been identified as a response biomarker for arsenic exposure in various types of cells, we were very interested: i) what is the role of HO-1 in *As*-induced nephrotoxicity (Gong et al. 2014) at clinically relevant doses? ii) what are the intricate molecular mechanisms involving in the regulation of HO-1 induction during *As* nephrotoxicity?

Furthermore, we have previously identified 2,3,5,6-tetramethylpyrazine (TMP), a compound extracted from the Chinese medicinal plant Ligusticum wallichi (Chuanxiong) as a protective agent against arsenic nephrotoxicity, which could attenuate ROS production, inflammation and cell death (Gong et al. 2014). One of the main aims of the current study was to further elucidate a potential relationship between HO-1 production and the renal protection by antioxidant TMP in arsenic nephrotoxicity, which is not well understood.

Arsenic response protein 2 (ARS2, also known as Srrt), was first isolated as a gene product conferring resistance to arsenite and arsenate in Ass/S5cell line (Rossman and Wang 1999). Based on the very limited published data, ARS2 has been shown to be essential for the development of plants and mammals, and also act as a transcriptional regulator of Sox2 in neural stem cell (Kiriyama et al. 2009; Wilson et al. 2008; Andreu-Agullo et al. 2012). However, the precise biological functions of ARS2 in mammalian are largely unknown (Wilson et al. 2008; Andreu-Agullo et al. 2012). The previous work from our laboratory has shown an upregulation of ARS2 expression in human neural stem cell after arsenic exposure (Ivanov and Hei 2013), which suggested ARS2 might be involved in arsenic-induced cytotoxicity and supported the previous suggestion that ARS2 has essential functions (Wilson et al. 2008). However, the signaling mechanism regulating ARS2 induction is still unclear, and a role of ARS2 in arsenic nephrotoxicity has not been reported so far.

In the present study, we have further investigated the potential relationships between HO-1induction, TMP-mediated renal protection and ARS2 expression in the suppression of arsenic nephrotoxicity.

Materials

All chemicals were purchased from Sigma (St. Louis, Mo., USA) unless otherwise stated. NF-κB inhibitor Bay 11-7082 (Bay), MAPK p38 inhibitor SB203580 (SB) and ERK inhibitor U0126 (U0) were obtained from Calbiochem (La Jolla, CA, USA) and JNK inhibitor SP600125 (SP) was obtained from Biomol (Plymouth Meeting, PA, USA).

Cell culture and treatment

The human proximal tubular cell line HK-2 (American Type Culture Collection, Manassas, VA, USA) was grown in culture medium (keratinocyte serum-free medium + 5 ng/ml epidermal growth factor and 50μg/ml bovine extract+ 100U/ml penicillin and 100μg/ml of streptomycin) at 37°C and 5% CO_2 humidified environment.

The next stock solutions were prepared: 50 mM sodium arsenite, antioxidant N-acetylcysteine (NAC, 10 mM), TMP (50 μM, 100μM) in PBS; NF-κB inhibitor Bay (5 μM), MAPK p38 inhibitor SB (10 μM), ERK inhibitor U0 (10μM) and JNK inhibitor SP (10 μM) in DMSO, and HO-1 inhibitor Zinc-Protoporphyrin (ZnPP, 2 μM) in methanol. NAC, TMP, and other inhibitors were added into media 30 min before As.

Intracellular ROS detection

Dihydroethidium (DHE, Invitrogen, Eugene, OR) method to detect intracellular superoxide production was used. After 24-h As treatment, cells were exposed to 2 μM DHE 45 minutes at 37 °C in the dark, then washed twice with PBS. Finally, Fluorescence-Activated Cell Sorter (FACS) analysis was performed (Becton Dickinson, Franklin Lakes, NJ) using the CellQuest program. Samples were analyzed in triplicates and all experiments were repeated 3 times independently.

Analyses of apoptosis by PI staining and FACS assay and TUNEL staining

Apoptotic cells were identified by diminished DNA content in the sub- G1 population of normal diploid cells by FACS assay after staining with propidium iodide (PI) (Gong et al. 2010). Approximately 20,000 counts were made for each sample. Finally, the data were collected and analyzed with CellQuest program combined with FACS machine. Apoptotic levels were calculated by evaluating the percentage of events accumulated in the sub-G 1 position. Samples were analyzed in triplicates and repeated 3 times.

To further confirm apoptotic cell death, terminal deoxynucleotidyl transferase-mediated dUTP-biotin nick-end labeling (TUNEL) staining was performed using a Click-iT TUNEL Alexa Fluor 488 Imaging Assay (Invitrogen, Grand Island, NY) according to the manufacturer's instructions except that PI replaced Hoechst 33342 to mount cells and label all nuclei. Stained nuclei were analyzed by a Nikon confocal microscope (Nikon TE200-C1) at 24 °C room temperature. TUNEL-positive cell numbers from 20 different fields (a total of 2000–2500 cells) were counted to get an average number of cells per field.

Mitochondrial network morphology assay

Mitochondrial network morphology and activity were visualized by using MitoTracker Green (Molecular Rrobes, Invitrogen). In brief, cells were grown on 6-well plate and incubated with 200 nM MitoTracker Green for another 20 min in 37 °C after 6h *As* treatment. After three time washes with PBS, cells were fixed with 4% paraformaldehyde. Confocal fluorescence microscopy images were captured and mitochondrial network morphology (tubular and non-tubular) was quantified by Image J software (NIH). Each treatment was randomly selected 20 non-contiguous fields for further observation and analysis, generally, each field containing 20–25 cells with mitochondrial networks. Percentages of normal (tubular) and abnormal (non-tubular) mitochondrial network morphologies were counted.

Mitochondrial function assay: Cytochrome c oxidase (Cox) and sucinate dehydrogenase (SDH) histochemistry

Cox and SDH histochemistry were monitored as described previously (Gong et al. 2014). In brief, cells were cultured on glass cover inside a 6-well plate. After 6h indicated treatment, cells on glass cover were allowed to dry at room temperature for 1 h, then followed by 15 min preincubation at room temperature with 1 mM $CoCl_2$ and 50μl DMSO in 50 mM Tris-HCL, pH 7.6, containing 10% sucrose. All samples were rinsed once in PBS and incubated for another 3 h with incubation medium (10 mg cytochrome *c*, 10 mg of DAB Hydrochloride, 2 mg of catalase and 25μl DMSO resolved in 10 ml 0.1 M phosphate buffer, pH 7.6). After further three times rinse, all samples were mounted on warm glycerin-gelatin and observed under Nikon LABOPHOT-2 microscope to capture images with SPOT Basic™ software. Quantification of histochemical staining was performed with Image J software (NIH). Camera light settings were standardized and color images were captured with 40x objective.

Western blotting

After the various treatments, whole cell lysates were prepared by incubation in RIPA buffer (Invitrogen). For nuclear transcription factor Nrf2 immunoblotting analysis, nuclear extracts were prepared using methods described previously (Schreiber et al. 1989). Protein concentrations were determined with Bio-Rad DC protein assay (Bio-Rad Laboratories, Calif., USA) using bovine serum albumin as the standard. The resulting protein samples underwent SDS-PAGE gel electrophoresis and were transferred to PVDF membrane.

The specific primary antibodies included the following rabbit Abs: anti-HO-1 (Enzo Life Sciences), anti-Bcl-xl (Cell Signaling), anti-Bax (Cell Signaling), anti-PARP (Cell Signaling), anti-pro Caspase-9 (Cell Signaling), anti-Nrf2 (Cell Signaling),anti-JNK (Cell Signaling), anti-phospho-JNK (Cell Signaling),anti-ERK (Cell Signaling), anti-phospho - ERK (Cell Signaling), anti-p38 MAPK (Cell Signaling), anti-phospho-p38 MAPK (Cell Signaling),anti-ARS2 (Santa Cruz), anti-histon H3(Cell signaling) and mouse anti-beta actin (Sigma).

Statistical analysis

The data were presented as means **±SD** for a minimum of three independent experiments. All comparisons were made using either One-way-ANOVA or a two tailed t-test analysis depending on how many conditions were compared in each experiment. One-way ANOVA was followed by Tukey's post hoc test. A value of $p<0.05$ was considered significant.

Results

2,3,5,6-tetramethylpyrazine (TMP) inhibited arsenic-induced ROS-dependent HO-1 expression

Arsenic (*As*) has been identified as inducer of heme oxygenase (HO)-1expression in many cells and tissues (Teng et al. 2013; Li et al. 2013). Consistent with these reports, we demonstrated that the induction of HO-1 protein expression was dose- and time-dependent in HK-2 cells after *As* exposure. Since the *As* dose range of 2.0 μM to 10 μM is successfully applied for treating acute promyelocytic leukemia (APL) and multiple myelomas (Ivanov and Hei 2005, 2004; Shen et al. 1997), we therefore choose this dose range for our present study. Furthermore, antioxidants N-acetylcystein (NAC) and TMP significantly inhibited arsenic-induced HO-1 expression (Fig. 1a and b). In contrast, aminoguanidine (AG), the iNOS inhibitor, failed in preventing HO-1 up-regulation (Fig. 1c–d).

Blocking HO-1 with ZnPP augmented *As*-induced apoptosis and ROS production

To verify the role of HO-1 in arsenic (*As*) nephrotoxicity, Zinc protoporphyrin (ZnPP), a known inhibitor of HO-1enzymatic activity, was used. Interestingly, ZnPP aggravated sodium arsenite (10 μM) induced cytotoxicity and apoptosis that was confirmed by increased percentage of cells accumulated in the sub-G1 position (35.7% versus 12.5%) determined by FACS analysis of PI stained cell nuclei (Fig. 2a and b) and by % TUNEL positive staining cells (Fig. 2 c and d).

Several studies have shown that the induction of HO-1 by As is ROS dependent (Fan et al. 2010; Teng et al. 2013). Our previous data have demonstrated that *As* exposure elevated ROS production in HK-2 cells (Gong et al. 2014). The present results demonstrate that ROS production is upregulated by 2.19 fold with 10 μM sodium arsenite treatment. Furthermore, combined treatments with ZnPP and 10 μM sodium arsenite resulted in a 5.35 fold increase in ROS production highlighting antioxidant role of HO-1 activation (Fig. 2e and f).

Inhibition of HO-1 activity with ZnPP augmented *As*-induced mitochondrial dysfunction

To further investigate the relationships among mitochondrial alterations, *As* nephrotoxicity, and blocking HO-1 activity, mitochondrial morphology was analyzed at the single cell level in Mito Tracker Green-stained HK2 cells. As shown in Fig. 3a, a large number of cells (84.6%) presented a normal (tubular) shape of mitochondrial network in the control group, while a number of cells with the abnormal (elongated or fragmented) mitochondrial networks was obviously increased in 10 μM sodium arsenite treated group, accordingly, the percentage of cells with tubular mitochondria in this group dropped to 35.7%. Augmented mitochondrial morphology changes were observed in ZnPP pretreatment group, whereas TMP and NAC pretreatment can effectively prevent this change in mitochondrial network morphology, and percentages of normal tubular morphology were 33.5%, 72.5% and 69.8% respectively (Fig. 3b).

Our previous study (Gong et al. 2014) indicated that sodium arsenite induced mitochondrial dysfunction in HK-2 cells, shown as strong loss of mitochondrial membrane potential and decreased Cox enzyme activity, which could be inhibited by NAC and TMP. In the present study, results of Cox enzyme histochemistry and mitochondrial membrane potential assay (data not shown) indicated that blocking HO-1 activity with ZnPP aggravated such a mitochondria dysfunction. Interestingly, the enzyme activity of SDH, or Complex II, encoded entirely by nuclear genome, was not significantly impaired by sodium arsenite treatment or ZnPP (Fig. 3c, d and e).

TMP prevented *As*-triggered the intrinsic apoptotic pathway activation in HK-2 cells

To explore whether sodium arsenite-induced apoptosis in HK-2 cells used the intrinsic mitochondrial pathway, the protein levels of Bax and Bcl-xl, a pro-apoptotic and an anti-apoptotic member, respectively, of the Bcl-2 family, were analyzed by western blotting. Sodium arsenite treatment for 24 h resulted in a reduction of anti-apoptotic Bcl-xl protein expression and an increase in the pro-apoptotic Bax protein expression (Fig. 4a). The decrease of pro-caspase-9 protein levels (that indicated on caspase-9 activation) and Caspase9/Caspase-3-dependent PARP1 cleavage induced by sodium arsenite treatment further demonstrated the involvement of intrinsic apoptotic pathway (Fig. 4a). Co-treatment with TMP (50 μM and 100 μM) prevented arsenic-triggered the intrinsic apoptotic pathway activation; and 100μM TMP showed higher protective efficiency (Fig. 4a).

TMP prevented *As*-induced HO-1 activation through inhibiting the activation of MAPKs/AP-1 pathways

Transcription factor AP-1 interacts with the corresponding binding site in the HO-1 gene promoter region and mediates HO-1 expression (Zhang et al. 2006). Furthermore, members

of the MAPKs family (ERK, JNK and p38) contributed to activation of AP-1 (Mossman et al. 2006). Thus, we next monitored impact of *As* on the activation of MAPKs family and AP-1 in HK-2 cells. As shown in Fig. 4b and Fig. 5a–b, *As* treatment induced MAPKs activation (the ERK, JNK, and p38 MAPK) 3 h after treatment in a dose-dependent manner. However, individual members showed different dynamic changes. Phospho JNK peaked at 3 h and showed the fastest down-regulation, phospho-ERK and phospho-p38 MAPK peaked at 6 h. Up-regulation of phospho-p38 MAPK was very durable and continued until 24 h. TMP co-treatment was very effective against *As*-induced ERK and MAPK p38 activation, but demonstrated only modest effects against JNK activation (Fig. 4b and 5a and b). Meanwhile, as an important member of AP-1 family, nuclear phospho-c-Jun protein expression increased after As exposure in a dose-dependent manner, while both 50μM and 100μM TMP efficiently inhibited *As*-induced phospho-c-Jun up-regulation; 100μM TMP demonstrated higher efficiency (Fig. 5c–d).

To further confirm a role of MAPKs in As-induced HO-1 expression, small molecule inhibitors of JNK, ERK and p38 MAPK were used. As shown in Fig. 6 a, b, and c, SB203580 (10 μM), an inhibitor of MAPK p38, and SP600125 (10 μM), a JNK inhibitor, efficiently down-regulated HO-1 protein expression induced by 3 h *As* exposure, while pretreatment with ERK inhibitor U0126 (10 μM) did not affected *As*-induced HO-1 expression, demonstrating the critical roles for MAPK p38 and JNK in *As*-induced induction of HO-1 protein expression. Meanwhile, both 50μM and 100μM TMP effectively inhibited *As*-induced-MAPKs activation, and compared with 50μM, 100μM TMP showed more efficient in inhibiting MAPKs activation (Fig. 4b and Fig. 5a–b).

TMP prevented *As*-induced HO-1 through inhibiting the activation of Nrf2 and NF-κB pathways

Two additional transcription factors, Nrf2 and NF-κB, control HO-1 gene and protein expression (Garnier et al. 2013; Wang et al. 2012; Lim et al. 2014). We monitored Nrf2 and phospho-NF-κB p65 (acive form) nuclear protein levels after *As* exposure of HK-2 cells. As shown in Fig. 6e, the nuclear Nrf2 protein was up-regulated in a dose-dependent manner as early as 3 h after *As* exposure and peaked at 6 h, while the increased expression lasted to 24 h. A similar dynamics was previously observed for nuclear phospho-NF-κB expression (Gong et al. 2014). To gain further insight into the relationship between activation of NF-κB p65 and HO-1 up-regulation induced by *As* exposure, we used co-treatment with Bay11-7082, an inhibitor of NF-κB, which selectively and irreversibly inhibits the inducible phosphorylation of IκB-α. As shown in Fig. 6 d, *As*-induced HO-1 protein expression was strongly down-regulated by 5 μM Bay11-7082. On the other hand, co-treatment with TMP partially suppressed *As*-induced Nrf2 upregulation (Fig. 6e). The similar effects of TMP on NF-κB activation was previously observed (Gong et al. 2014).

TMP prevented *As*-induced up-regulation of ARS2 expression in HK-2 cells

To elucidate a role of transcription factor ARS2 in arsenic-induced kidney injury, we determined *As*-induced protein expression of ARS2 in HK-2 cells. As shown in Fig. 7a, As treatment increased ARS2 protein expression, such an up-regulation was peaking at 6 h and then gradually decreased. TMP (100μM) efficiently inhibited *As*-induced ARS2 up-

regulation. Next, to achieve the purpose whether MAPKs and NF-κB contributed to *As*-mediated ARS2 induction, we used co-treatment with As and specific molecule inhibitors. SB203580 (an inhibitor of p38) and U0126 (an inhibitor of ERK), but not SP600125 (an inhibitor of JNK), obviously inhibited *As*-induced ARS2 up-regulation at 6 h, which indicated MAPK p38 and ERK acted at the upstream of ARS2 expression (Fig. 7c–e). Additionally, as Fig. 7b demonstrates, Bay11-7082 reversed the effect of *As* on ARS2, which indicated that *As*-induced ARS2 up-regulation was also modulated by NF-κB activation in HK-2 cells.

Discussion

Our previous study (Gong et al. 2014) identified that sodium arsenite at a clinically relevant dose also might be a risk factor for kidney, while TMP could prevent such an *As*-induced nephrotoxicity by reducing ROS production, preventing mitochondria dysfunction, and suppressing activation of pro-inflammatory signals, including β-catenin, NF-κB, TNF-α and cyclooxygenase-2 (COX2). However, the precise renal-cellular adaptive mechanism and antioxidant-mediated protective responses against arsenic exposure with clinical relevant dose are still not clear. In the present study, we revealed that clinical relevant concentrations of sodium arsenite induced dose-dependent and specific activation of MAPKs that further activated transcription factors Nrf2, NF-κB, and AP-1/cJun, which then control the downstream antioxidant response of HO-1 in HK-2 cells. Additionally, we observed the up-regulation of transcription factor ARS2 expression in this processes, which strongly supported the previous speculation about essential function of ARS2 (Wilson et al. 2008). Interestingly, TMP inhibited *As*-induced Nrf2, AP-1 and MAPKs family activations, accordingly, and reduced HO-1 and ARS2 expressions, which might contribute to its nephroprotective effects.

HO-1 has been identified as a biological hallmark of cells in response to unfavorable environment, including oxidative stress (Teng et al. 2013; Lee et al. 2012). In our previous study (Gong et al. 2014), *As* exposure dramatically increased cellular ROS production in HK-2 cells, and antioxidant NAC and TMP efficiently prevented *As*-induced cytotoxicity and ROS production. In the present study, the involvement of oxidative stress in *As*-induced nephrotoxicity was further investigated by monitoring HO-1 expression. As Fig. 1a–b shown, we identified the induced-HO-1 protein expression after *As* exposure was in a dose- and time-dependent manner, whereas the treatment of TMP and antioxidant NAC blocked *As*-induced HO-1 expression. Such a result also suggested the tight relationship between HO-1 induction and intracellular ROS production after arsenite exposure in HK-2 cells. Interestingly, aminoguanidine (AG), the inhibitor of iNOS, has no effect on the expression of HO-1 in response to *As*, which suggested *As*-induced HO-1 production might mainly be mediated by ROS, not nitrostative stress.

Furthermore, a role of HO-1 in *As*-induced nephrotoxicity was investigated using ZnPP, a known inhibitor of HO-1. Blocking *As*-induced HO-1enzymatic activity by ZnPP resulted in decreased cell viability (data not shown), and promoted *As*-induced programmed cell death ascertained by increased sub-G1 phase and TUNEL-positive cells. Accordingly, cellular ROS production achieved 5.35 fold increasing, significantly higher than after *As* treatment.

Our previous data have confirmed that mitochondrial damage was involved in *As*-induced nephrotoxicity (Gong et al. 2014). In the present study, we found that blocking HO-1 further exacerbated *As*-induced mitochondrial injury and respiratory chain damage, ascertained as a decrease in the number of tubular mitochondria and down-regulation in Cox expression. All these data mentioned above strongly demonstrated that HO-1 played a protective role in *As*-induced nephrotoxicity, and blocking HO-1 augmented *As*-induced cell death, ROS production and mitochondrial injury. In the other studies, HO-1 also has been shown to protect kidney against several acute kidney injury (AKI) (Billings et al. 2014; Miyagi et al. 2014; Goodman et al. 2007).

Nuclear factor erythroid derived-2 (Nrf2) is involved in one of the most important cellular defense mechanisms against oxidative stress by regulating cytoprotective enzymes expressions, for example, HO-1 (Zhang et al. 2012; Kilic et al. 2013). Furthermore, Nrf2 has been viewed as a protective protein against genotoxic damage. Consistent with the above views, there is evidence that Nrf2 could protect human bladder urothelial cells (Wang et al. 2007) from *As* toxicity and attenuate hyperglycemia-induced kidney injury in diabetic mice (Li et al. 2011). In contrast, the present study demonstrated that in spite of Nrf2 and Nrf2-regulated cytoprotective HO-1 gene were activated after *As* exposure at a clinically relevant dose, such an increased expression of Nrf2 and HO-1 failed to rescue HK-2 cells from *As*-induced cytotoxicity.

Similar results were observed in *As*-treated oral squamous cells, which might suggest Nrf2 and HO-1-dependent protection was overwhelmed by *As* cytotoxicity (Zhang et al. 2012). Indeed, while up-regualtion of HO-1 is regarded as cytoprotective under various experiments conditions, it can be non-sufficient to fully recover cells from oxidative damage, as shown in our study and other publication (Wang et al. 2012).

Although many studies highlighted the importance of Nrf2 pathway in *As*-induced HO-1 expression in different cell lines (Li et al. 2013; Pi et al. 2008), indeed, the mechanisms underlying HO-1 induction are regulated by the complex signaling network. In the present study, we observed a discrepancy between Nrf2 and HO-1 protein expression after *As* exposure in HK-2 cells: *As*-induced HO-1 expression was in a dose- and time-dependent manner, whereas *As*-induced Nrf2 expression peaked at 6 h, and then degraded gradually. Such discrepancy also suggested that *As* might induce HO-1 gene expression through Nrf2-independent pathways. The previous research suggested that Nrf2 played essential role for HO-1 induction only in the early and transient phase after *As* exposure in embryonic fibroblasts (Li et al. 2013).

HO-1 induction is tightly regulated primarily at the transcriptional level, Nrf2 recruited BRG1 to the HO-1 enhancers and the promoter, meanwhile, activator protein-1 (AP-1) and NF-κB located in HO-1 gene promoter region (Zhang et al. 2006). Our previous data identified that *As* with clinical dose induced phospho-NF-κB p65 nuclear protein (active form) expression in HK-2 cells (Gong et al. 2014). In the present study, to gain insight into the functional relationship between NF-κB activation and HO-1 up-regulation in response to *As*, HK-2 cells were pre-incubated with Bay11-7082, a specific inhibitor of NF-κB, for 30 min followed by 10 μM sodium arsenite treatment for 6 h. Fig. 6b showed co-treatment of

10 μM sodium arsenite and Bay substantially inhibited HO-1 expression as compared with *As* alone, which further indicated the induction of HO-1 expression in *As*-induced nephrotoxicity is through multiple pathways and, at least partially, through NF-κB activation. AP-1 is another transcription factor that could control the HO -1 gene expression (Zhang et al. 2006). In addition, MAPKs contributed to AP-1 induction (Hsieh et al. 2014). Thus, we next monitored *As* impact on the activations of MAPKs and AP-1, and investigated the relationship between MAPKs and HO-1 expression in HK-2 cells. As Fig. 4b and 5 shown, arsenic exposure resulted in MAPKs family activations, which is very consistent to the other studies (Wang et al. 2012; Kang et al. 2003), but such activation seemed to be cell- and species-dependent (Wang et al. 2012). For example, *As* exposure only strongly activated p38 MAPK in normal human lung fibroblast, and did not activate ERK and JNK (Wang et al. 2013a).

Additionally, the present study established that arsenic exposure within clinical relevant dose could activate AP-1 family member c-Jun in HK-2 cells (Fig. 5c–d) that is very consistent to the previous study (Deshane et al. 2010) demonstrating its role for HO-1 induction in renal epithelial cell. Interestingly, only SB203580 (an inhibitor of p38) and SP600125 (an inhibitor of JNK), but not U0126 (an inhibitor of ERK), efficiently attenuated *As*-induced HO-1 production that confirmed only p38 MAPK and JNK, but not ERK, contributed to the up-regulation of HO-1after As exposure in HK2 cells.

Taken together, our present data demonstrated that the regulation mechanisms of *As*-induced HO-1 expression were performed through multiple signal pathways, Nrf2, NF-κB, AP-1, p38 MAPK and JNK.

In our previous study, TMP could reverse the *As*-induced a sequence of proinflammatory signal regulators, including NF-κB, p38 MAPK, beta-catenin and COX2 and protect HK-2 cells against *As*-induced programmed cell death (autophagy and apoptosis) (Gong et al. 2014). In current study, another novel finding is the demonstration that TMP could also suppress the activations of Nrf2, AP-1, JNK and ERK after *As* exposure, accordingly, block HO-1 protein expression in HK-2 cells. Furthermore, such protection was performed by preventing *As*-triggered activation of the intrinsic apoptotic pathway. Interestingly, TMP was also found to inhibit proliferation of human promyelocytic leukemia cell line HL-60 (Wu et al. 2012).

So far, there were no related reports, which focused on the effects of *As* on induction of transcription factor ARS2 in *As*-induced nephrotoxicity. In the present study, *As* treatment increased ARS2 protein expression. Interestingly, the dynamic change of *A*s-induced ARS2 expression showed a similar manner with COX2 (Gong et al. 2014). Similar to the effects on MAPKs, TMP efficiently inhibited ARS2 up-regulation. Nevertheless, attention should be paid to the very interesting phenomenon, demonstrating that Bay11-7082 (a specific inhibitor of NF-κB), SB203580 (an inhibitor of p38), and U0126 (an inhibitor of ERK), but not SP600125 (an inhibitor of JNK), attenuate the effects of *As* on ARS2 expression. This indicated that *As*-induced ARS2 up-regulation was modulated by the activations of NF-κB, p38 MAPK and ERK, but not JNK in HK-2 cells. To our knowledge, this is the first report demonstrating that ARS2 involved in *As*-induced nephrotoxicity and it was regulated by p38

MAPK, ERK and NF-κB. Further studies focusing on the potential function of ARS2 in *As*-induced nephrotoxicity is worthy of attention.

Although it is not clear which role ARS2 plays in *As*-induced nephrotoxicity, but given ARS2 and HO-1 sharing the similar regulation mechanism, we thus hypothesize that ARS2 and HO-1 might mediate cell survival in response to *As* treatment in HK-2 cells. Previous report also has revealed that Ars2 played a role in RNA interference regulation during cell proliferation and in the ability of mammalian cells to proliferate (Gruber et al. 2009) that also gave the supporting evidence for our speculation of ARS2 mediating cell survival in As-induced nephrotoxicity in HK-2 cells.

In summary, the present study further confirmed that arsenic treatment at clinically relevant dose result in renal damage, additionally, the activations of Nrf2, AP-1, MAPKs family and ARS2 involved in such a nephrotoxicity. Furthermore, the cytoprotective HO-1 induction after *As* exposure in HK-2 cells is mediated by multiple pathways, including Nrf2, NF-κB, AP-1, p38 MAPK and JNK. The current data also demonstrated TMP efficiently reverse *As*-induced Nrf2, NF-κB, AP-1, MAPKs family activations, and block the according HO-1 and ARS2 expressions. Although further studies are required, we can still propose TMP could be effective in the treatment of arsenic-induced nephrotoxicity.

Acknowledgments

The authors would like to thank Drs. Preety Sharma, Erik Young, Bo Zhang, Gangkun Lin, Wupeng Liao, Hongning Zhou and Winsome Walker for advice and helpful discussion. This work was supported by Environmental Center Grant P30 ES009089, NIH Grant P01 CA049062 and National Natural Science Foundation of China Grant 81573936 and 81373614.

Abbreviations

AG	aminoguanidine
AKI	acute kidney injury
ARS2	Arsenic response protein 2
As	Arsenic
Bay	Bay 11-7082
CKD	chronic kidney disease
DHE	Dihydroethidium
FACS	fluorescence-activated cell sorter
HO-1	heme oxygenase-1
MAPK	mitogen-activated protein kinase
Nrf2	nuclear factor erythroid derived-2
NAC	N-acetylcysteine

NF-κB	nuclear factor-κB
PARP	poly ADP-ribose polymerase
PI	propidium iodide
ROS	reactive oxygen species
SB	SB203580
SDH	sucinate dehydrogenase
SP	SP600125
TMP	Tetramethylpyrazine
TUNEL	terminal deoxynucleotidyl transferase-mediated dUTP-biotin nick-end labeling
U0	U0126
ZnPP	Zinc protoporphyrin

References

Andreu-Agullo C, Maurin T, Thompson CB, Lai EC. Ars2 maintains neural stem-cell identity through direct transcriptional activation of Sox2. Nature. 2012; 481 (7380):195–198. nature10712 [pii]. DOI: 10.1038/nature10712 [PubMed: 22198669]

Billings IF, Yu C, Byrne JG, Petracek MR, Pretorius M. Heme Oxygenase-1 and Acute Kidney Injury following Cardiac Surgery. Cardiorenal Med. 2014; 4(1):12–21. crm-0004-0012 [pii]. DOI: 10.1159/000357871 [PubMed: 24847330]

Chang CF, Liu XM, Peyton KJ, Durante W. Heme oxygenase-1 counteracts contrast media-induced endothelial cell dysfunction. Biochem Pharmacol. 2014; 87 (2):303–311. S0006-2952(13)00717-X [pii]. DOI: 10.1016/j.bcp.2013.11.002 [PubMed: 24239896]

Chen JW, Chen HY, Li WF, Liou SH, Chen CJ, Wu JH, Wang SL. The association between total urinary arsenic concentration and renal dysfunction in a community-based population from central Taiwan. Chemosphere. 2011; 84 (1):17–24. S0045-6535(11)00256-6 [pii]. DOI: 10.1016/j.chemosphere.2011.02.091 [PubMed: 21458841]

Chen WJ, Huang YL, Shiue HS, Chen TW, Lin YF, Huang CY, Lin YC, Han BC, Hsueh YM. Renin-angiotensin-aldosterone system related gene polymorphisms and urinary total arsenic is related to chronic kidney disease. Toxicol Appl Pharmacol. 2014; 279 (2):95–102. S0041-008X(14)00208-7 [pii]. DOI: 10.1016/j.taap.2014.05.011 [PubMed: 24907556]

Deshane J, Kim J, Bolisetty S, Hock TD, Hill-Kapturczak N, Agarwal A. Sp1 regulates chromatin looping between an intronic enhancer and distal promoter of the human heme oxygenase-1 gene in renal cells. J Biol Chem. 2010; 285 (22):16476–16486. M109.058586 [pii]. DOI: 10.1074/jbc.M109.058586 [PubMed: 20351094]

Fan SF, Chao PL, Lin AM. Arsenite induces oxidative injury in rat brain: synergistic effect of iron. Ann N Y Acad Sci. 2010; 1199:27–35. NYAS5170 [pii]. DOI: 10.1111/j.1749-6632.2009.05170.x [PubMed: 20633106]

Garnier N, Petruccelli LA, Molina MF, Kourelis M, Kwan S, Diaz Z, Schipper HM, Gupta A, del Rincon SV, Mann KK, Miller WH Jr. The novel arsenical Darinaparsin circumvents BRG1-dependent, HO-1-mediated cytoprotection in leukemic cells. Leukemia. 2013; 27 (11):2220–2228. leu201354 [pii]. DOI: 10.1038/leu.2013.54 [PubMed: 23426167]

Gong X, Celsi G, Carlsson K, Norgren S, Chen M. N-acetylcysteine amide protects renal proximal tubular epithelial cells against iohexol-induced apoptosis by blocking p38 MAPK and iNOS

signaling. Am J Nephrol. 2010; 31 (2):178–188. 000268161 [pii]. DOI: 10.1159/000268161 [PubMed: 20016144]

Gong X, Ivanov VN, Davidson MM, Hei TK. Tetramethylpyrazine (TMP) protects against sodium arsenite-induced nephrotoxicity by suppressing ROS production, mitochondrial dysfunction, pro-inflammatory signaling pathways and programed cell death. Arch Toxicol. 2014; doi: 10.1007/s00204-014-1302-y

Goodman AI, Olszanecki R, Yang LM, Quan S, Li M, Omura S, Stec DE, Abraham NG. Heme oxygenase-1 protects against radiocontrast-induced acute kidney injury by regulating anti-apoptotic proteins. Kidney Int. 2007; 72 (8):945–953. 5002447 [pii]. DOI: 10.1038/sj.ki.5002447 [PubMed: 17667987]

Gruber JJ, Zatechka DS, Sabin LR, Yong J, Lum JJ, Kong M, Zong WX, Zhang Z, Lau CK, Rawlings J, Cherry S, Ihle JN, Dreyfuss G, Thompson CB. Ars2 links the nuclear cap-binding complex to RNA interference and cell proliferation. Cell. 2009; 138 (2):328–339. S0092-8674(09)00507-8 [pii]. DOI: 10.1016/j.cell.2009.04.046 [PubMed: 19632182]

Hsieh HL, Lin CC, Chan HJ, Yang CM. c-Src-dependent EGF receptor transactivation contributes to ET-1-induced COX-2 expression in brain microvascular endothelial cells. J Neuroinflammation. 2014; 9:152. 1742–2094-9-152 [pii]. doi: 10.1186/1742-2094-9-152 [PubMed: 22747786]

Huang JX, Kaeslin G, Ranall MV, Blaskovich MA, Becker B, Butler MS, Little MH, Lash LH, Cooper MA. Evaluation of biomarkers for in vitro prediction of drug-induced nephrotoxicity: comparison of HK-2, immortalized human proximal tubule epithelial, and primary cultures of human proximal tubular cells. Pharmacol Res Perspect. 2015; 3 (3):e00148.doi: 10.1002/prp2.148 [PubMed: 26171227]

Ivanov VN, Hei TK. Arsenite sensitizes human melanomas to apoptosis via tumor necrosis factor alpha-mediated pathway. J Biol Chem. 2004; 279(21):22747–22758. M314131200 [pii]. DOI: 10.1074/jbc.M314131200 [PubMed: 15028728]

Ivanov VN, Hei TK. Combined treatment with EGFR inhibitors and arsenite upregulated apoptosis in human EGFR-positive melanomas: a role of suppression of the PI3K-AKT pathway. Oncogene. 2005; 24 (4):616–626. 1208125 [pii]. DOI: 10.1038/sj.onc.1208125 [PubMed: 15580309]

Ivanov VN, Hei TK. Induction of apoptotic death and retardation of neuronal differentiation of human neural stem cells by sodium arsenite treatment. Exp Cell Res. 2013; 319 (6):875–887. S0014-4827(12)00476-4 [pii]. DOI: 10.1016/j.yexcr.2012.11.019 [PubMed: 23219847]

Kang SH, Song JH, Kang HK, Kang JH, Kim SJ, Kang HW, Lee YK, Park DB. Arsenic trioxide-induced apoptosis is independent of stress-responsive signaling pathways but sensitive to inhibition of inducible nitric oxide synthase in HepG2 cells. Exp Mol Med. 2003; 35 (2):83–90. 200304304 [pii]. DOI: 10.1038/emm.2003.12 [PubMed: 12754411]

Kilic U, Kilic E, Tuzcu Z, Tuzcu M, Ozercan IH, Yilmaz O, Sahin F, Sahin K. Melatonin suppresses cisplatin-induced nephrotoxicity via activation of Nrf-2/HO-1 pathway. Nutr Metab (Lond). 2013; 10 (1):7. 1743-7075-10-7 [pii]. doi: 10.1186/1743-7075-10-7 [PubMed: 23311701]

Kiriyama M, Kobayashi Y, Saito M, Ishikawa F, Yonehara S. Interaction of FLASH with arsenite resistance protein 2 is involved in cell cycle progression at S phase. Mol Cell Biol. 2009; 29 (17):4729–4741. MCB.00289-09 [pii]. DOI: 10.1128/MCB.00289-09 [PubMed: 19546234]

Lee JE, Park JH, Shin IC, Koh HC. Reactive oxygen species regulated mitochondria-mediated apoptosis in PC12 cells exposed to chlorpyrifos. Toxicol Appl Pharmacol. 2012; 263 (2):148–162. S0041-008X(12)00264-5 [pii]. DOI: 10.1016/j.taap.2012.06.005 [PubMed: 22714038]

Li B, Li X, Zhu B, Zhang X, Wang Y, Xu Y, Wang H, Hou Y, Zheng Q, Sun G. Sodium arsenite induced reactive oxygen species generation, nuclear factor (erythroid-2 related) factor 2 activation, heme oxygenase-1 expression, and glutathione elevation in Chang human hepatocytes. Environ Toxicol. 2013; 28 (7):401–410. DOI: 10.1002/tox.20731 [PubMed: 21809430]

Li H, Zhang L, Wang F, Shi Y, Ren Y, Liu Q, Cao Y, Duan H. Attenuation of glomerular injury in diabetic mice with tert-butylhydroquinone through nuclear factor erythroid 2-related factor 2-dependent antioxidant gene activation. Am J Nephrol. 2011; 33 (4):289–297. 000324694 [pii]. DOI: 10.1159/000324694 [PubMed: 21389693]

Lim JL, Wilhelmus MM, de Vries HE, Drukarch B, Hoozemans JJ, van Horssen J. Antioxidative defense mechanisms controlled by Nrf2: state-of-the-art and clinical perspectives in

neurodegenerative diseases. Arch Toxicol. 2014; 88 (10):1773–1786. DOI: 10.1007/s00204-014-1338-z [PubMed: 25164826]

Michael HA. Geochemistry. An arsenic forecast for China. Science. 2013; 341 (6148):852–853. 341/6148/852 [pii]. DOI: 10.1126/science.1242212 [PubMed: 23970688]

Miyagi MY, Seelaender M, Castoldi A, de Almeida DC, Bacurau AV, Andrade-Oliveira V, Enjiu LM, Pisciottano M, Hayashida CY, Hiyane MI, Brum PC, Camara NO, Amano MT. Long-term aerobic exercise protects against cisplatin-induced nephrotoxicity by modulating the expression of IL-6 and HO-1. PLoS One. 2014; 9(10):e108543. PONE-D-14-31578 [pii]. doi: 10.1371/journal.pone.0108543 [PubMed: 25272046]

Mossman BT, Lounsbury KM, Reddy SP. Oxidants and signaling by mitogen-activated protein kinases in lung epithelium. Am J Respir Cell Mol Biol. 2006; 34 (6):666–669. 2006-0047SF [pii]. DOI: 10.1165/rcmb.2006-0047SF [PubMed: 16484683]

Peraza MA, Carter DE, Gandolfi AJ. Toxicity and metabolism of subcytotoxic inorganic arsenic in human renal proximal tubule epithelial cells (HK-2). Cell Biol Toxicol. 2003; 19 (4):253–264. [PubMed: 14686617]

Peraza MA, Cromey DW, Carolus B, Carter DE, Gandolfi AJ. Morphological and functional alterations in human proximal tubular cell line induced by low level inorganic arsenic: evidence for targeting of mitochondria and initiated apoptosis. J Appl Toxicol. 2006; 26 (4):356–367. DOI: 10.1002/jat.1149 [PubMed: 16773642]

Pi J, Diwan BA, Sun Y, Liu J, Qu W, He Y, Styblo M, Waalkes MP. Arsenic-induced malignant transformation of human keratinocytes: involvement of Nrf2. Free Radic Biol Med. 2008; 45 (5):651–658. S0891-5849(08)00303-1 [pii]. DOI: 10.1016/j.freeradbiomed.2008.05.020 [PubMed: 18572023]

Rodriguez-Lado L, Sun G, Berg M, Zhang Q, Xue H, Zheng Q, Johnson CA. Groundwater arsenic contamination throughout China. Science. 2013; 341 (6148):866–868. 341/6148/866 [pii]. DOI: 10.1126/science.1237484 [PubMed: 23970694]

Rossman TG, Wang Z. Expression cloning for arsenite-resistance resulted in isolation of tumor-suppressor fau cDNA: possible involvement of the ubiquitin system in arsenic carcinogenesis. Carcinogenesis. 1999; 20 (2):311–316. [PubMed: 10069470]

Ruiz-Hernandez A, Kuo CC, Rentero-Garrido P, Tang WY, Redon J, Ordovas JM, Navas-Acien A, Tellez-Plaza M. Environmental chemicals and DNA methylation in adults: a systematic review of the epidemiologic evidence. Clin Epigenetics. 2015; 7(1):55. 55 [pii]. doi: 10.1186/s13148-015-0055-7 [PubMed: 25984247]

Schreiber E, Matthias P, Muller MM, Schaffner W. Rapid detection of octamer binding proteins with ‘mini-extracts’, prepared from a small number of cells. Nucleic Acids Res. 1989; 17 (15):6419. [PubMed: 2771659]

Shen ZX, Chen GQ, Ni JH, Li XS, Xiong SM, Qiu QY, Zhu J, Tang W, Sun GL, Yang KQ, Chen Y, Zhou L, Fang ZW, Wang YT, Ma J, Zhang P, Zhang TD, Chen SJ, Chen Z, Wang ZY. Use of arsenic trioxide (As2O3) in the treatment of acute promyelocytic leukemia (APL): II. Clinical efficacy and pharmacokinetics in relapsed patients. Blood. 1997; 89 (9):3354–3360. [PubMed: 9129042]

Teng YC, Tai YI, Lee YH, Lin AM. Role of HO-1 in the arsenite-induced neurotoxicity in primary cultured cortical neurons. Mol Neurobiol. 2013; 48 (2):281–287. DOI: 10.1007/s12035-013-8492-9 [PubMed: 23824679]

Wang J, Dore S. Heme oxygenase-1 exacerbates early brain injury after intracerebral haemorrhage. Brain. 2007; 130 (Pt 6):1643–1652. 130/6/1643 [pii]. DOI: 10.1093/brain/awm095 [PubMed: 17525142]

Wang L, Kou MC, Weng CY, Hu LW, Wang YJ, Wu MJ. Arsenic modulates heme oxygenase-1, interleukin-6, and vascular endothelial growth factor expression in endothelial cells: roles of ROS, NF-kappaB, and MAPK pathways. Arch Toxicol. 2012; 86 (6):879–896. DOI: 10.1007/s00204-012-0845-z [PubMed: 22488045]

Wang Q, Wu L, Wang J. Reciprocal regulation of cyclooxygenase 2 and heme oxygenase 1 upon arsenic trioxide exposure in normal human lung fibroblast. J Biochem Mol Toxicol. 2013a; 27 (6):323–329. DOI: 10.1002/jbt.21491 [PubMed: 23649692]

Wang S, Wei Q, Dong G, Dong Z. ERK-mediated suppression of cilia in cisplatin-induced tubular cell apoptosis and acute kidney injury. Biochim Biophys Acta. 2013b; 1832 (10):1582–1590. S0925-4439(13)00185-3 [pii]. DOI: 10.1016/j.bbadis.2013.05.023 [PubMed: 23727409]

Wang XJ, Sun Z, Chen W, Eblin KE, Gandolfi JA, Zhang DD. Nrf2 protects human bladder urothelial cells from arsenite and monomethylarsonous acid toxicity. Toxicol Appl Pharmacol. 2007; 225 (2): 206–213. S0041-008X(07)00330-4 [pii]. DOI: 10.1016/j.taap.2007.07.016 [PubMed: 17765279]

Wilson MD, Wang D, Wagner R, Breyssens H, Gertsenstein M, Lobe C, Lu X, Nagy A, Burke RD, Koop BF, Howard PL. ARS2 is a conserved eukaryotic gene essential for early mammalian development. Mol Cell Biol. 2008; 28 (5):1503–1514. MCB.01565-07 [pii]. DOI: 10.1128/MCB.01565-07 [PubMed: 18086880]

Wu Y, Xu Y, Shen Y, Wang C, Guo G, Hu T. Tetramethylpyrazine potentiates arsenic trioxide activity against HL-60 cell lines. Braz J Med Biol Res. 2012; 45(3):187–196. S0100-879X2012007500017 [pii]. [PubMed: 22331136]

Yu M, Xue J, Li Y, Zhang W, Ma D, Liu L, Zhang Z. Resveratrol protects against arsenic trioxide-induced nephrotoxicity by facilitating arsenic metabolism and decreasing oxidative stress. Arch Toxicol. 2013; 87 (6):1025–1035. DOI: 10.1007/s00204-013-1026-4 [PubMed: 23471352]

Zhang J, Ohta T, Maruyama A, Hosoya T, Nishikawa K, Maher JM, Shibahara S, Itoh K, Yamamoto M. BRG1 interacts with Nrf2 to selectively mediate HO-1 induction in response to oxidative stress. Mol Cell Biol. 2006; 26 (21):7942–7952. MCB.00700-06 [pii]. DOI: 10.1128/MCB.00700-06 [PubMed: 16923960]

Zhang X, Su Y, Zhang M, Sun Z. Opposite effects of arsenic trioxide on the Nrf2 pathway in oral squamous cell carcinoma in vitro and in vivo. Cancer Lett. 2012; 318 (1):93–98. S0304-3835(11)00742-7 [pii] . DOI: 10.1016/j.canlet.2011.12.005 [PubMed: 22155346]

Zheng L, Kuo CC, Fadrowski J, Agnew J, Weaver VM, Navas-Acien A. Arsenic and Chronic Kidney Disease: A Systematic Review. Curr Environ Health Rep. 2014; 1 (3):192–207. DOI: 10.1007/s40572-014-0024-x [PubMed: 25221743]

Zheng LY, Umans JG, Tellez-Plaza M, Yeh F, Francesconi KA, Goessler W, Silbergeld EK, Guallar E, Howard BV, Weaver VM, Navas-Acien A. Urine arsenic and prevalent albuminuria: evidence from a population-based study. Am J Kidney Dis. 2013; 61 (3):385–394. S0272-6386(12)01259-0 [pii]. DOI: 10.1053/j.ajkd.2012.09.011 [PubMed: 23142528]

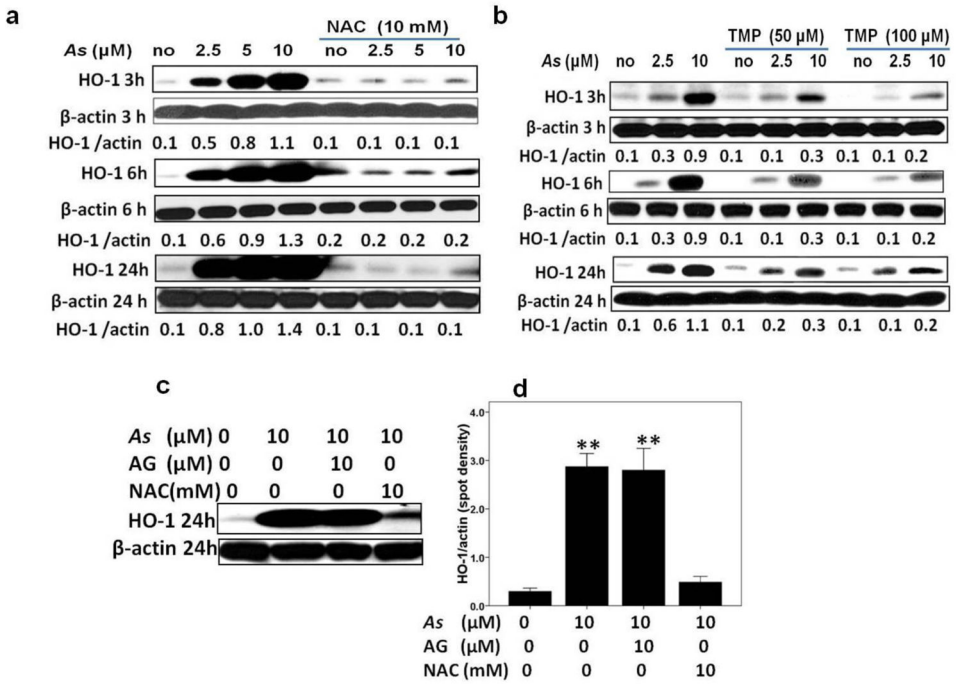

Fig. 1. TMP inhibited arsenic-induced ROS dependent HO-1 expression in HK-2 cells

(a–b) HK-2 cells were exposed to sodium arsenite at indicated doses for 3, 6, and 24 h alone or in a combination with either 10 mM NAC or 50μM-100 μM TMP. Arsenite (*As*) exposure induced HO-1 protein expression in a dose- and time-dependent manner, whereas NAC and TMP pretreatment sufficiently blocked HO-1 up-regulation. (c–d) Compared with 10 mM NAC, 10μM AG, the inhibitor of iNOS, failed in preventing HO-1 up-regulation. β-Actin was used as loading control. Quantitative densitometry of protein bands was performed. Values are mean ± SD (n=3), (**) $p<0.01$ vs. control.

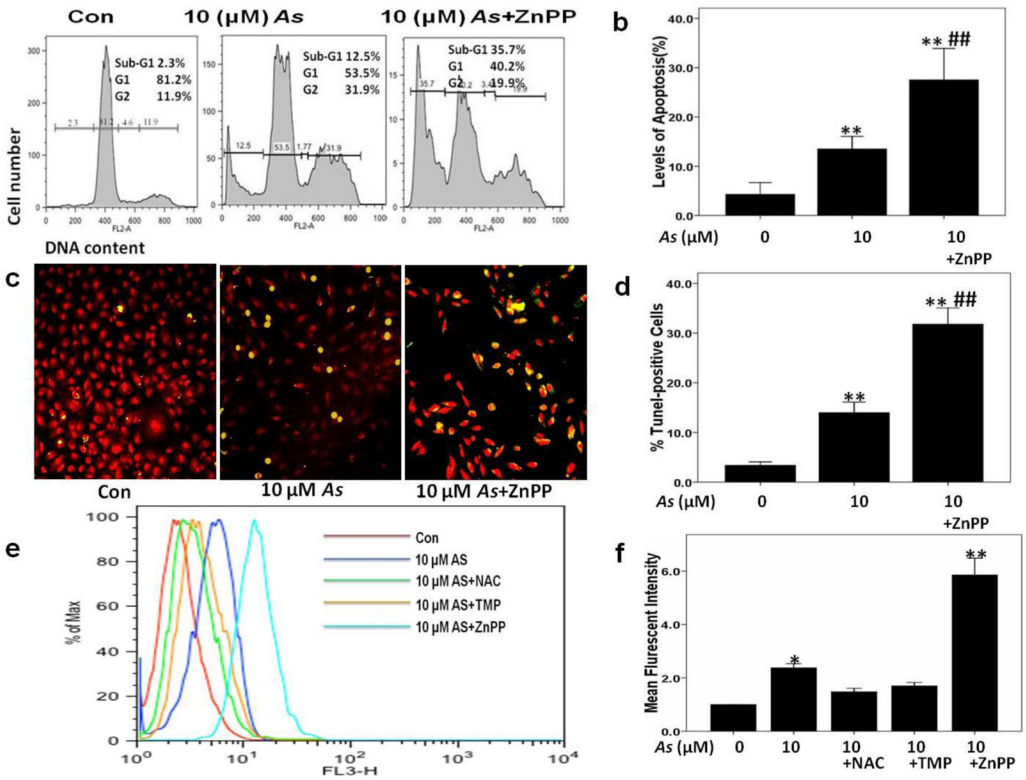

Fig. 2. Blocking HO-1 activity with ZnPP augmented arsenic-induced apoptosis and ROS production

Apoptosis levels and intracellular ROS production were measured 24 h after arsenic (*As*) treatment with or without 2 μM ZnPP pretreatment of HK-2 cells. (a–b) Levels of apoptosis were calculated by evaluating the percentage of cells accumulated in the sub-G1 position after PI staining DNA. (c–d) Apoptosis was determined by TUNEL staining, and average percentages of TUNLE-positive cells were assessed in each group. (e–f) 100 μM TMP and 10 mM NAC inhibited *As*-induced ROS generation at 24 h, while 2 μM ZnPP augmented ROS generation. Values are mean ± SD (n=3), (*) $p<0.05$ vs Con; (**) $p<0.01$ vs Con; (##) $p<0.01$ vs. 10μM *As*.

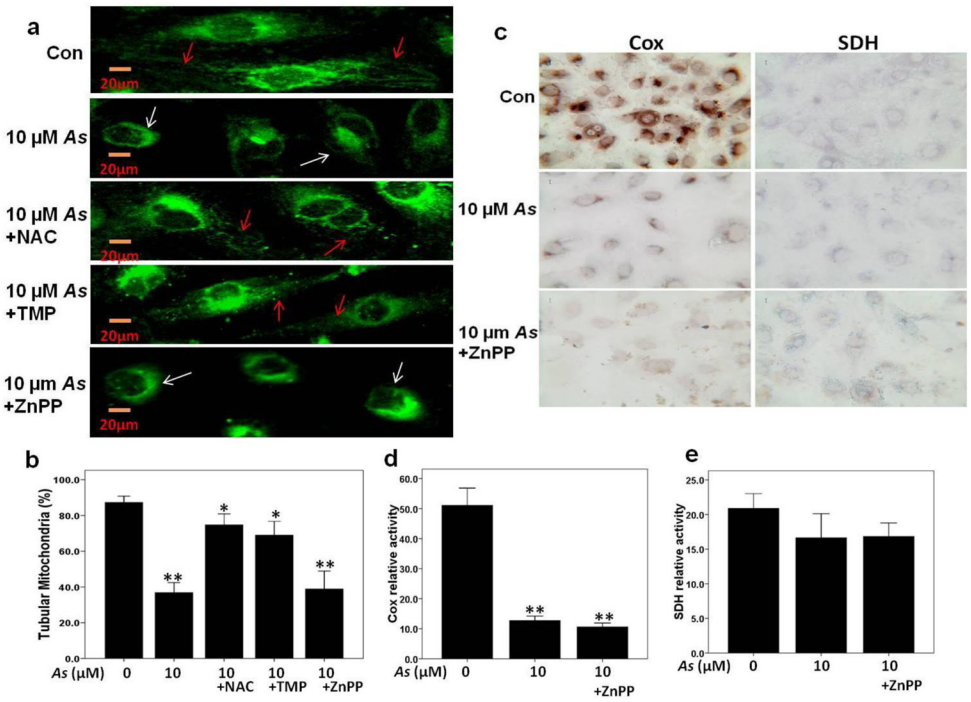

Fig. 3. Blocking HO-1 with ZnPP augmented arsenic-induced mitochondrial dysfunction

(a–b) Mitochondrial morphology was determined at the single cell level in Mito Tracker Green-stained HK2 cells, and the cell number with different mitochondrial morphology (normal as tubular with red arrow, elongated or fragmented with white arrow) was counted in each group. (c–d) *As*-induced mitochondrial dysfunction was verified by a decreased cytochrome *c* oxidase (Cox) histochemical staining. (c and e) Sucinate dehydrogenase (SDH) histochemical staining. Values are mean ± SD (n=3), (*) $p<0.05$ vs Con, (**) $p<0.01$ vs Con.

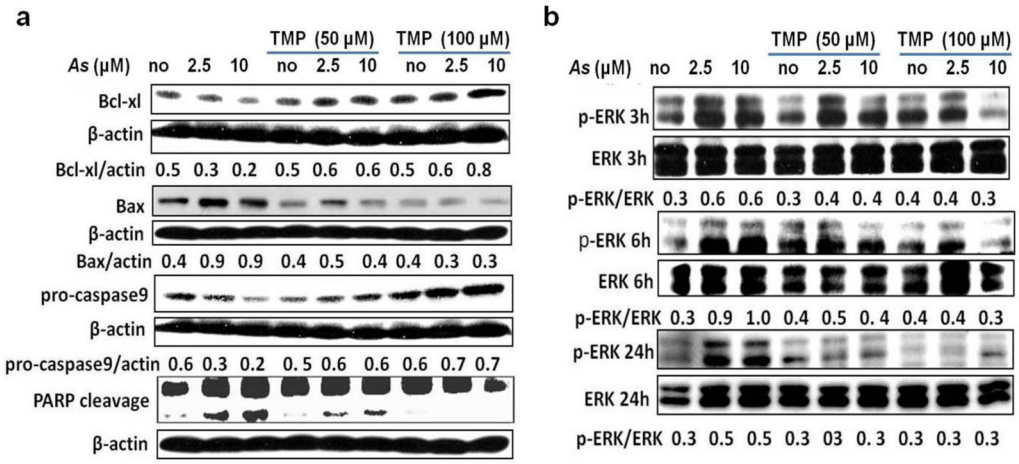

Fig. 4. TMP prevented arsenic-triggered activations of the intrinsic apoptotic pathway and ERK pathway in HK-2 cells

(a) *As* treatment (24 h) increased protein levels of pro-apoptotic Bax and pro-caspase9 expressions and decreased levels of anti-apoptotic Bcl-xl, and PARP cleavage, while TMP (50 μM and 100 μM) pretreatment prevented *As*-triggered the intrinsic apoptotic pathway activation. (b) *As*-induced ERK activation was verified by increased level of phospho-Thr202/Tyr204 ERK (p-ERK) expression, which was inhibited by TMP pretreatment. β-actin was used as loading control. Values are mean ± SD (n=3).

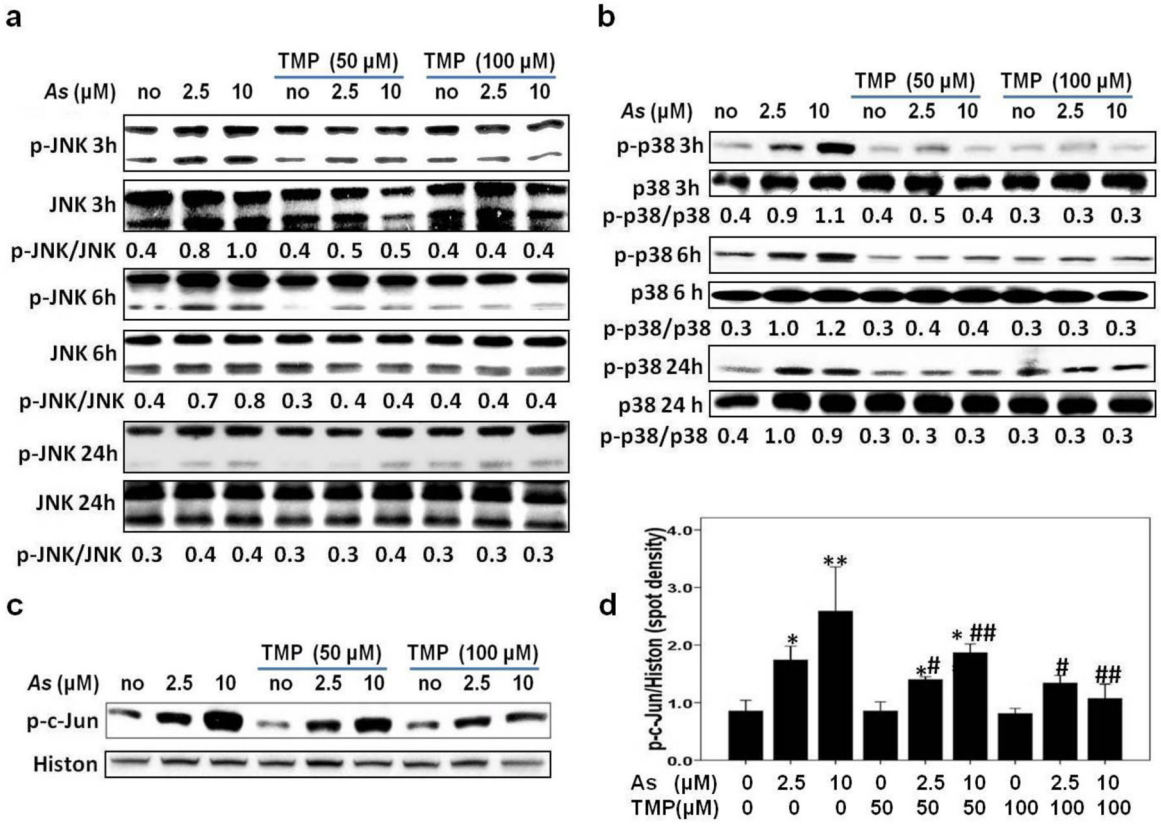

Fig. 5. TMP prevented arsenic-triggered activations of p38 MAPK, JNK and c-Jun pathways in HK-2 cells

As-induced JNK (a) and p38 MAPK (b) activations were verified by increased levels of phospho-Thr183/Tyr185 MAPK (p-JNK) and phospho-Thr180/Tyr182 p38 MAPK (p-p38) expression respectively, which were inhibited by TMP pretreatment. (c and d) 6-h *As* exposure resulted in nuclear phospho-c-Jun up-regulation, while both 50μM and 100μM TMP efficiently inhibited As-induced nuclear c-Jun activation. Histone H3 (Histon) and β-actin were used as loading controls for nuclear and total proteins, respectively. Values are mean ± SD (n=3); (*) $p<0.05$ vs Con; (**) $p<0.01$ vs Con; (#) $p<0.05$ vs. 2.5μM As, (##) $p<0.01$ vs. 10μM As.

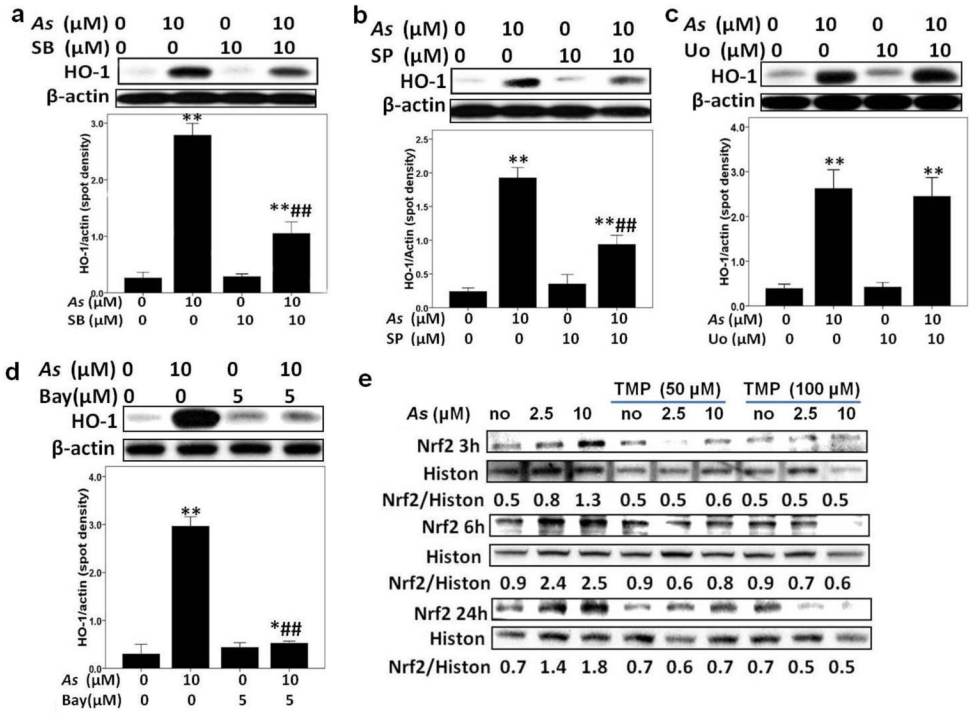

Fig. 6. TMP prevented arsenic-triggered activation of Nrf2 pathway in HK-2 cells, meanwhile, arsenic-induced HO-1 was Nrf2, NF-κB, p38 MAPK and JNK dependent

SB203580 (SB) (a), SP600125 (SP) (b), and Bay11-7082 (Bay) (d), not UO126 (UO) (c), inhibited arsenic-induced HO-1 expressions in HK-2 cells. Additionally, TMP inhibited arsenic-induced up-regulation of nuclear Nrf2 in HK-2 cells (e). Histone H3 (Histon) and β-actin were used as loading controls for nuclear and total proteins, respectively. Values are mean ± SD (n=3), (*) $p<0.05$ vs Con; (**) $p<0.01$ vs Con; (##) $p<0.01$ vs 10μM As.

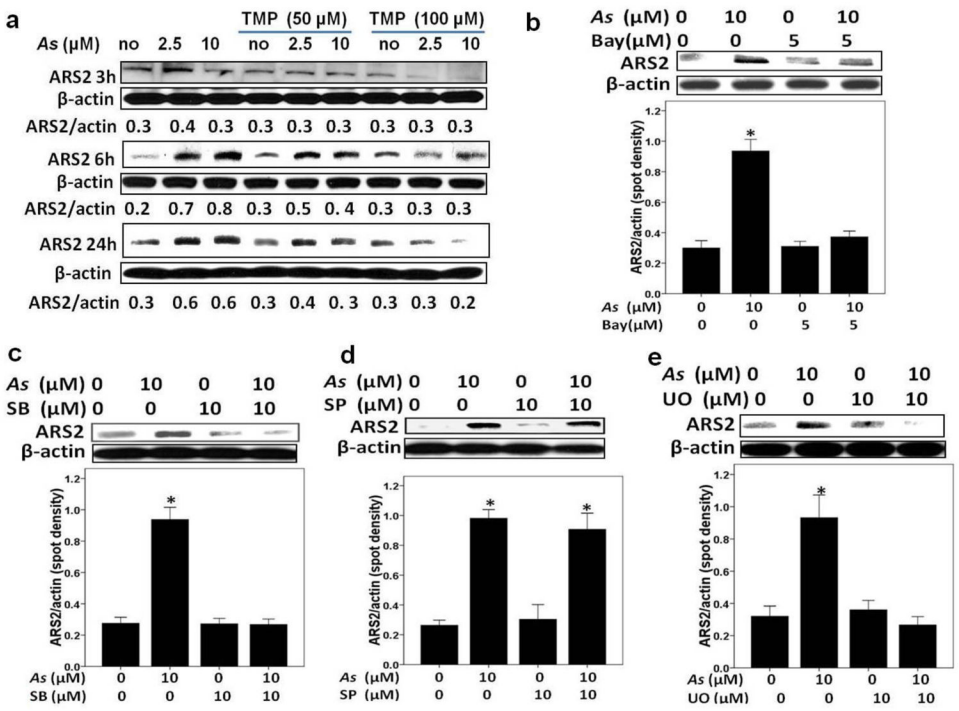

Fig. 7. Arsenic-triggered ARS2 expression was NF-κB, p38 MAPK and ERK dependent in HK-2 cells

Pretreatment of TMP (a), Bay11-7082 (Bay) (b), SB203580 (SB) (c) and UO126 (UO) (e), while not SP600125 (SP) (d), efficiently inhibited *As*-induced ARS2 expression. β-actin was used as loading control for total proteins. Values are mean ± SD (n=3), (*) $p<0.05$ vs. Con.